Progress In Electromagnetics Research B, Vol. 3, 271–281, 2008

DESIGN OF BAND-PASS WAVEGUIDE FILTER USING FREQUENCY SELECTIVE SURFACES LOADED WITH SURFACE MOUNT CAPACITORS BASED ON SPLIT-FIELD UPDATE FDTD METHOD

S. M. Amjadi and M. Soleimani

Iran University of Science and Technology
Iran

Abstract—A new band-pass narrow-band, miniaturized and single resonance within a wide range of frequency band frequency selective surface structure with lumped capacitors suitable for low frequency and narrowband waveguide filter applications is presented. The filter structure consists of five unit cells in one direction with notch square ring elements each consists of two lumped capacitors placed on the transverse plane of the rectangular waveguide. To reduce the simulation time in design procedure, split-field update FDTD method is used for the analysis of the unit cell of the analogous infinite frequency selective surface at different oblique incidence of plane waves to predict the FSS performance in the waveguide. As an application, a waveguide filter has been designed to be used in an easy to fabricate and inexpensive S-band band-pass filter. By using lumped capacitors, several undesirable higher order resonance frequencies near the dominant resonance frequency are eliminated and the waveguide filter dimensions are reduced considerably in one direction compared with the analogous waveguide filter without lumped capacitors.

1. INTRODUCTION

In the past years, waveguide filters by using periodic structures with periodicity in the longitudinal direction of the waveguide , to attain a band-pass or band-stop frequency characteristic have been introduced [1, 2]. Frequency selective surfaces (FSSs) have also been used for their state of being special to act as metallic-dielectric spatial filters in order to design dual-frequency waveguide filters [3, 4]. Recently, filter designing by placing FSSs transversally into the waveguide to achieve more advantages including miniaturization, being

lightweight and easy to be fabricated, have been presented [5, 6]. Making multiple images of the FSS, the metallic walls of the waveguide cause the FSS unit cell to be infinite [4, 6]. The fundamental mode of a rectangular waveguide can be considered as two transverse electric uniform plane waves (in the longitudinal direction of the waveguide) bouncing back and forth at oblique incidence between the waveguide smaller size side walls having 180° phase reversal with the propagation angle that depends on frequency and can be expressed as [7]:

$$\theta_{inc}(Degree) = \frac{180}{\pi}\cos^{-1}\left(\sqrt{\left(\frac{2\pi f}{c}\right)^2 - \left(\frac{\pi}{a}\right)^2}\Big/\left(\frac{2\pi f}{c}\right)\right) \quad (1)$$

In this equation, c, a and f are the free-space velocity of light, the widest dimension of the rectangular waveguide, and the operating frequency respectively. Therefore, if the FSS exhibits stable resonance with respect to polarization and incidence angle of plane waves, the waveguide filter characteristics will be more symmetric around the resonance frequency and more similar to the frequency response of the analogous infinite FSS. When used as a band-pass filter in the waveguide, a conventional FSS may pass some higher order resonance frequencies that is not favorable. Furthermore the unit cell size in a conventional FSS is large for low frequency bands. Lumped elements including inductors and capacitors at microwave and millimeter wave frequencies are now available and can be used in high frequency band periodic structures such as frequency selective surfaces [8] and artificial magnetic conductors. In this paper, lumped capacitors are used in the FSS structure as an alternative approach to achieve all these features simultaneously. In order to reduce the simulation time in the waveguide filter design procedure, first the unit cell size of the analogous infinite FSS is analyzed. Because these structures are needed to be analyzed over a wide range of frequency band, fast time domain methods are preferred rather than the frequency domain methods. Several time domain methods have been presented for the analysis of periodic structures. Split-field update FDTD method [9] is one of the most powerful methods used for the analysis of periodic structures at oblique incidence. Here, lumped elements formulations are incorporated in this method formulation based on [10] and the proposed structure is analyzed using this method. Finally a band-pass waveguide filter is designed using the presented FSS structure.

2. METHOD FORMULATION

The proposed method for including lumped elements in the split-field method is presented in this section for 3D case. Here a parallel RLC in considered. When a parallel RLC is inserted into the FDTD space lattice, the Maxwell's curl $\vec{H}$ equation becomes [10]:

$$\nabla \times \vec{H} = \frac{\partial \vec{D}}{\partial t} + \vec{J}_{Res} + \vec{J}_{Cap} + \vec{J}_{Induc} \tag{2}$$

$$J_{z-Res} = \frac{dz}{Rdxdy} E_z \tag{3}$$

$$J_{z-Cap} = \frac{Cdz}{dxdy} \left(\frac{\partial E_z}{\partial t} \right) \tag{4}$$

$$J_{z-Induc} = \frac{dz}{Ldxdy} \int_0^t E_z dt \tag{5}$$

A periodic structure in y and z directions is considered and lumped elements are x, y or z-directed that is defined by an index. Using (2)–(5), the 3D transformed field equations with lumped elements for P components are given by:

$$\begin{aligned} \frac{\varepsilon_r}{c}\frac{\partial P_x}{\partial t} + \sigma\eta_0 P_x &= \frac{\partial Q_z}{\partial y} - \frac{\partial Q_y}{\partial z} - \frac{\overline{k}_y}{c}\frac{\partial Q_z}{\partial t} + \frac{\overline{k}_z}{c}\frac{\partial Q_y}{\partial t} - \frac{dx}{c\varepsilon_0 R_x dydz} P_x \\ &\quad - \frac{C_x dx}{c\varepsilon_0 dy\, dz}\left(\frac{\partial P_x}{\partial t}\right) - \frac{c\mu_0 dx}{L_x\, dy\, dz}\int_0^t P_x\, dt \end{aligned} \tag{6}$$

$$\begin{aligned} \frac{\varepsilon_r}{c}\frac{\partial P_y}{\partial t} + \sigma\eta_0 P_y &= -\frac{\partial Q_z}{\partial x} + \frac{\partial Q_x}{\partial z} - \frac{\overline{k}_z}{c}\frac{\partial Q_x}{\partial t} - \frac{dy}{c\varepsilon_0 R_y dxdz} P_y \\ &\quad - \frac{C_y dy}{c\varepsilon_0 dx\, dz}\left(\frac{\partial P_y}{\partial t}\right) - \frac{c\mu_0 dy}{L_y dxdz}\int_0^t P_y\, dt \end{aligned} \tag{7}$$

$$\begin{aligned} \frac{\varepsilon_r}{c}\frac{\partial P_z}{\partial t} + \sigma\eta_0 P_z &= \frac{\partial Q_y}{\partial x} - \frac{\partial Q_x}{\partial y} + \frac{\overline{k}_y}{c}\frac{\partial Q_x}{\partial t} - \frac{dz}{c\varepsilon_0 R_z dxdy} P_z \\ &\quad - \frac{C_z dz}{c\varepsilon_0 dx\, dy}\left(\frac{\partial P_z}{\partial t}\right) - \frac{c\mu_0 dz}{L_z\, dx\, dy}\int_0^t P_z\, dt \end{aligned} \tag{8}$$

$$\frac{\mu_r}{c}\frac{\partial Q_x}{\partial t} + \frac{\sigma^{\cdot}}{\eta_0} Q_x = -\frac{\partial P_z}{\partial y} + \frac{\partial P_y}{\partial z} + \frac{\overline{k}_y}{c}\frac{\partial P_z}{\partial t} - \frac{\overline{k}_z}{c}\frac{\partial P_y}{\partial t} \tag{9}$$

$$\frac{\mu_r}{c}\frac{\partial Q_y}{\partial t}+\frac{\sigma^{\cdot}}{\eta_0}Q_y = \frac{\partial P_z}{\partial x}+\frac{\partial P_x}{\partial z}+\frac{\overline{k}_z}{c}\frac{\partial P_x}{\partial t} \tag{10}$$

$$\frac{\mu_r}{c}\frac{\partial Q_z}{\partial t}+\frac{\sigma^{\cdot}}{\eta_0}Q_z = -\frac{\partial P_y}{\partial x}+\frac{\partial P_x}{\partial y}-\frac{\overline{k}_y}{c}\frac{\partial P_x}{\partial t} \tag{11}$$

By defining new variables, the extra time derivatives on the right hand side can be eliminated. In [9] the fields in the directions of the structure periodicities are split into two components. Here, UPML absorbing boundary condition is used. For similar periodic boundary conditions for "a" portions of the fields in the UPML region and non-UPML region, the field components in the direction of the structure periodicities are split into three components as for the UPML region [11]. New variables must be defined as follows:

$$P_x = P_{xa}+\frac{\overline{k}_z}{\varepsilon_r+\frac{C_x dx}{\varepsilon_0 dydz}}Q_y-\frac{\overline{k}_y}{\varepsilon_r+\frac{C_x dx}{\varepsilon_0 dydz}}Q_z;\ Q_x=Q_{xa}-\frac{\overline{k}_z}{\mu_r}P_y+\frac{\overline{k}_y}{\mu_r}P_z \tag{12}$$

$$P_y = P_{ya}+P_{yb}-\frac{\overline{k}_z}{\varepsilon_r+\frac{C_y dy}{\varepsilon_0 dxdz}}Q_x;\ Q_y = Q_{ya}+Q_{yb}+\frac{\overline{k}_z}{\mu_r}P_x \tag{13}$$

$$P_z = P_{za}+P_{zb}+\frac{\overline{k}_y}{\varepsilon_r+\frac{C_z dz}{\varepsilon_0 dxdy}}Q_x;\ Q_z = Q_{za}+Q_{zb}-\frac{\overline{k}_y}{\mu_r}P_x \tag{14}$$

Substituting these variables into the systems (6)–(11) results in:

$$\begin{aligned}
&\left(\frac{\varepsilon_r}{c}+\frac{C_x dx}{c\varepsilon_0 dydz}\right)\frac{\partial P_{xa}}{\partial t}+\left(\sigma\eta_0+\frac{dx}{c\varepsilon_0 R_x dydz}\right)P_{xa}\\
&= \frac{\partial Q_z}{\partial y}-\frac{\partial Q_y}{\partial z}+\frac{\sigma\eta_0+\frac{dx}{c\varepsilon_0 R_x dydz}}{\varepsilon_r+\frac{C_x dx}{\varepsilon_0 dydz}}\overline{k}_y Q_z-\frac{\sigma\eta_0+\frac{dx}{c\varepsilon_0 R_x dydz}}{\varepsilon_r+\frac{C_x dx}{\varepsilon_0 dydz}}\overline{k}_z Q_y\\
&\quad -\frac{c\mu_0 dx}{L_x dydz}\int_0^t P_{xa}dt-\frac{\overline{k}_z}{\varepsilon_r+\frac{C_x dx}{\varepsilon_0 dydz}}\frac{c\mu_0 dx}{L_x dydz}\int_0^t Q_y dt\\
&\quad -\frac{\overline{k}_y}{\varepsilon_r+\frac{C_x dx}{\varepsilon_0 dydz}}\frac{c\mu_0 dx}{L_x dydz}\int_0^t Q_z dt
\end{aligned} \tag{15}$$

$$\begin{aligned}
&\left(\frac{\varepsilon_r}{c}+\frac{C_y dy}{c\varepsilon_0 dxdz}\right)\frac{\partial P_{ya}}{\partial t}+\left(\sigma\eta_0+\frac{dy}{c\varepsilon_0 R_y dxdz}\right)P_{ya}\\
&= -\frac{\partial Q_z}{\partial x}-\frac{c\mu_0 dy}{L_y dxdz}\int_0^t P_{ya}dt
\end{aligned} \tag{16}$$

$$\left(\frac{\varepsilon_r}{c}+\frac{C_y dy}{c\varepsilon_0 dxdz}\right)\frac{\partial P_{yb}}{\partial t}+\left(\sigma\eta_0+\frac{dy}{c\varepsilon_0 R_y dxdz}\right)P_{yb}$$

$$= \frac{\partial Q_x}{\partial z}+\frac{\sigma\eta_0+\frac{dy}{c\varepsilon_0 R_y dxdz}}{\varepsilon_r+\frac{C_y dy}{\varepsilon_0 dxdz}}\overline{k}_z Q_x-\frac{c\mu_0 dy}{L_y dxdz}\int_0^t P_{yb}dt$$

$$-\frac{\overline{k}_z}{\varepsilon_r+\frac{C_y dy}{\varepsilon_0 dxdz}}\frac{c\mu_0 dy}{L_y dxdz}\int_0^t Q_x dt \tag{17}$$

$$\left(\frac{\varepsilon_r}{c}+\frac{C_z dz}{c\varepsilon_0 dxdy}\right)\frac{\partial P_{za}}{\partial t}+\left(\sigma\eta_0+\frac{dz}{c\varepsilon_0 R_z dxdy}\right)P_{za}$$

$$= \frac{\partial Q_y}{\partial x}-\frac{c\mu_0 dz}{L_z dxdy}\int_0^t P_{za}dt \tag{18}$$

$$\left(\frac{\varepsilon_r}{c}+\frac{C_z dz}{c\varepsilon_0 dxdy}\right)\frac{\partial P_{zb}}{\partial t}+\left(\sigma\eta_0+\frac{dz}{c\varepsilon_0 R_z dxdy}\right)P_{zb}$$

$$= -\frac{\partial Q_x}{\partial y}-\frac{\sigma\eta_0+\frac{dz}{c\varepsilon_0 R_z dxdy}}{\varepsilon_r+\frac{C_z dz}{\varepsilon_0 dxdy}}\overline{k}_y Q_x-\frac{c\mu_0 dz}{L_z dxdy}\int_0^t P_{zb}dt$$

$$-\frac{\overline{k}_y}{\varepsilon_r+\frac{C_z dz}{\varepsilon_0 dxdy}}\frac{c\mu_0 dz}{L_z dxdy}\int_0^t Q_x dt \tag{19}$$

$$\frac{\mu_r}{c}\frac{\partial Q_{xa}}{\partial t}+\frac{\sigma^{\cdot}}{\eta_0}Q_{xa} = -\frac{\partial P_z}{\partial y}+\frac{\partial P_y}{\partial z}-\frac{\sigma^{\cdot}\overline{k}_y}{\eta_0\mu_r}P_z+\frac{\sigma^{\cdot}\overline{k}_z}{\eta_0\mu_r}P_y \tag{20}$$

$$\frac{\mu_r}{c}\frac{\partial Q_{ya}}{\partial t}+\frac{\sigma^{\cdot}}{\eta_0}Q_{ya} = -\frac{\partial P_z}{\partial x} \tag{21}$$

$$\frac{\mu_r}{c}\frac{\partial Q_{yb}}{\partial t}+\frac{\sigma^{\cdot}}{\eta_0}Q_{yb} = -\frac{\partial P_x}{\partial z}-\frac{\sigma^{\cdot}\overline{k}_y}{\eta_0\mu_r}P_z-\frac{\sigma^{\cdot}\overline{k}_z}{\eta_0\mu_r}P_x \tag{22}$$

$$\frac{\mu_r}{c}\frac{\partial Q_{za}}{\partial t}+\frac{\sigma^{\cdot}}{\eta_0}Q_{za} = -\frac{\partial P_y}{\partial x} \tag{23}$$

$$\frac{\mu_r}{c}\frac{\partial Q_{zb}}{\partial t}+\frac{\sigma^{\cdot}}{\eta_0}Q_{zb} = \frac{\partial P_x}{\partial y}_z+\frac{\sigma^{\cdot}\overline{k}_y}{\eta_0\mu_r}P_x \tag{24}$$

Once "a" and "b" portions are updated, the new values of the x-

components are found by:

$$\left(1-\frac{\overline{k}_y^2}{\mu_r\left(\varepsilon_r+\frac{C_z dz}{\varepsilon_0 dxdy}\right)}-\frac{\overline{k}_z^2}{\mu_r\left(\varepsilon_r+\frac{C_y dy}{\varepsilon_0 dxdz}\right)}\right)Q_x$$
$$= Q_{xa}-\frac{\overline{k}_z}{\mu_r}\left(P_{ya}+P_{yb}\right)+\frac{\overline{k}_y}{\mu_r}\left(P_{za}+P_{zb}\right) \quad (25)$$

$$\left(1-\frac{\overline{k}_y^2}{\mu_r\left(\varepsilon_r+\frac{C_x dx}{\varepsilon_0 dydz}\right)}-\frac{\overline{k}_z^2}{\mu_r\left(\varepsilon_r+\frac{C_x dx}{\varepsilon_0 dydz}\right)}\right)P_x$$
$$= P_{xa}+\frac{\overline{k}_z}{\varepsilon_r+\frac{C_x dx}{\varepsilon_0 dydz}}\left(Q_{ya}+Q_{yb}\right)-\frac{\overline{k}_y}{\varepsilon_r+\frac{C_x dx}{\varepsilon_0 dydz}}\left(Q_{za}+Q_{zb}\right) \quad (26)$$

The remaining field components are given by:

$$P_y=P_{ya}+P_{yb}-\frac{\overline{k}_z}{\left(\varepsilon_r+\frac{C_y dy}{\varepsilon_0 dxdz}\right)}Q_x;\ P_z=P_{za}+P_{zb}+\frac{\overline{k}_y}{\left(\varepsilon_r+\frac{C_z dz}{\varepsilon_0 dxdy}\right)}Q_x \quad (27)$$

$$Q_y=Q_{ya}+Q_{yb}+\frac{\overline{k}_z}{\mu_r}P_x;\ Q_z=Q_{za}+Q_{zb}-\frac{\overline{k}_y}{\mu_r}P_x \quad (28)$$

The stability factor condition does not change and is explained in [9].

3. FILTER DESIGN AND NUMERICAL RESULTS

In order to design the waveguide filter, first the analogous infinite band-pas FSS used in the waveguide filter is analyzed using split-field method to predict the waveguide filter performance. The unit cell of the FSS structure designed at the 3.15 GHz with four 2 mm × 1 mm ceramic chip capacitors is shown in Fig. 1. All capacitors are 1 pf. A dielectric substrate with $\varepsilon_r = 2.5$ and $h = 1$ mm is used. The transmission coefficient of this structure for different incidence angles of TE_x plane wave with z-directed electric field component is illustrated in Fig. 2. As it shows, the structure exhibits stable resonance in different incidence angles. The maximum shift in the resonance frequency is less than 0.1%. The transmission coefficient of this structure at normal incidence from 1GHz to 14 GHz is shown in Fig. 3. The only resonance frequency in this frequency band is 3.15 GHz. Therefore, several undesirable higher order resonance frequencies near the dominant resonance frequency are eliminated. In fact, not only the unit cell size of a conventional FSS with notch square ring elements without

lumped capacitors at this frequency band is larger by a factor of about four in comparison with the structure shown in Fig. 1, but also a conventional notch square ring FSS is transparent at some higher order resonance frequencies near the dominant resonance frequency that is not favourable. Furthermore, the maximum resonance frequency shift for different incidence angles for this structure is much less than the resonance frequency shift of a conventional FSS with notch square ring.

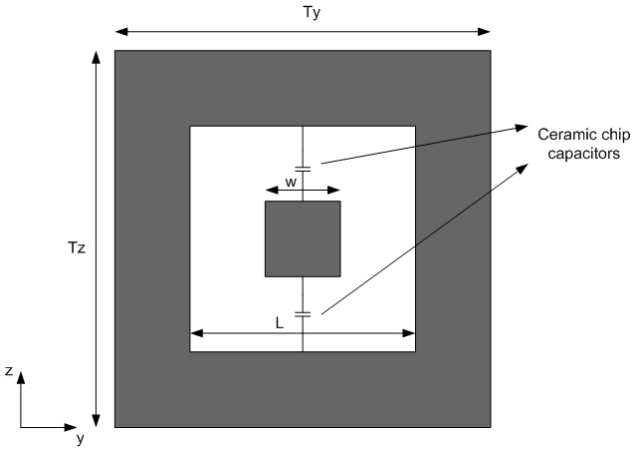

Figure 1. The Geometry of notch square ring FSS with ceramic chip capacitors. $(Ty,\, Tz,\, L,\, W) = (10, 10, 6, 2)$ mm.

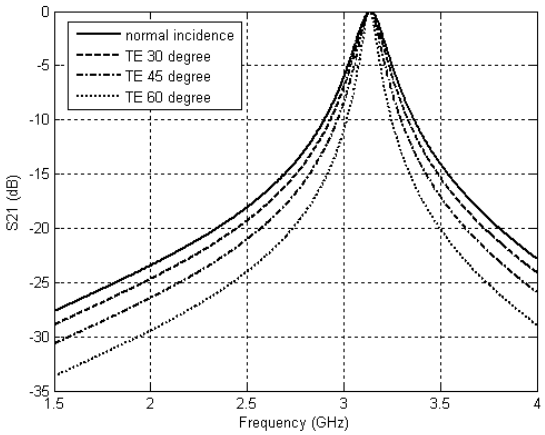

Figure 2. Transmission coefficient of the FSS structure shown in Fig. 1 for different plan waves.

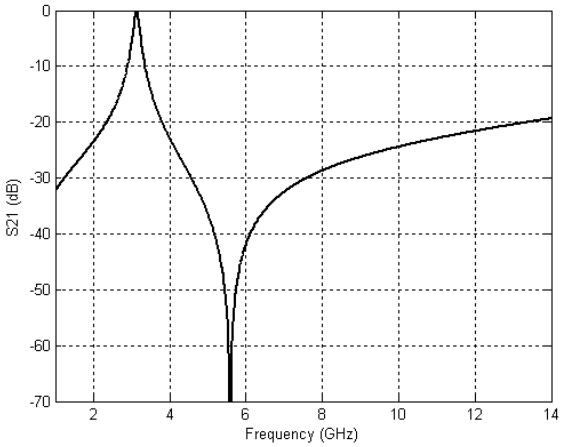

Figure 3. Transmission coefficient of the FSS structure shown in Fig. 1 for normal incidence.

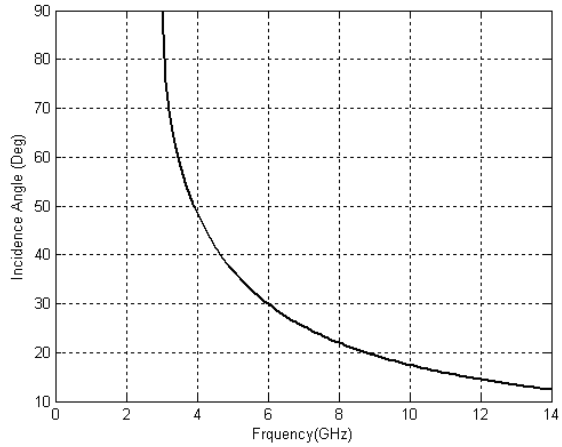

Figure 4. The incidence angle of the corresponding plane wave versus frequency for the dominant mode of the waveguide shown in Fig. 5.

The waveguide filter setup is shown in Fig. 5. The widest side of the waveguide size is chosen so that the waveguide cut-off frequency is below the FSS resonance frequency. Therefore, five FSS unit cells can be placed in the transverse plane of the rectangular waveguide. Fig. 4 illustrates the incidence angle of the corresponding plane wave bouncing at oblique incidence between the waveguide smaller size lateral walls versus frequency for the dominant mode of this waveguide

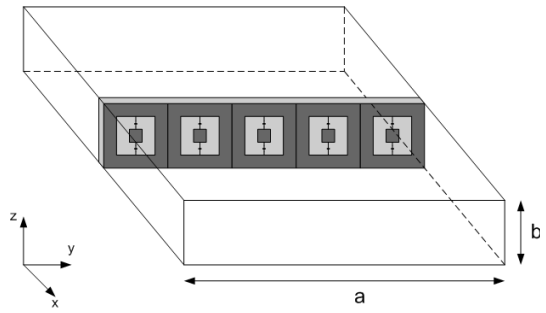

Figure 5. Setup of the filter within the waveguide. ($a = 50\,\text{mm}$, $b = 10\,\text{mm}$).

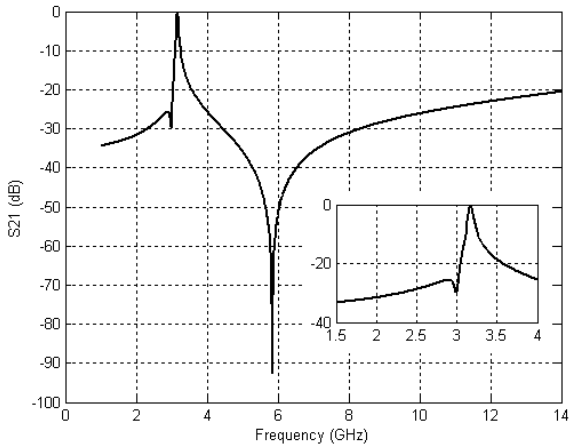

Figure 6. Transmission coefficient for the dominant mode of the waveguide filter shown in Fig. 5.

obtained by (1). The transmission coefficient of the waveguide filter from 1GHz to 14 GHz is shown in Fig. 6. As it shows, the resonance occurs at 3.17 GHz and there is no other resonance frequency in this frequency band. The frequency response of the waveguide filter at each frequency is similar to the frequency response of the analogous infinite FSS exited by a plane wave with the corresponding incidence angle showed in Fig. 4. If a conventional notch square ring FSS without lumped capacitors is used for the design of a waveguide filter at this frequency, the size of the narrower waveguide side increased about 80% in comparison with the waveguide shown in Fig. 5, because the FSS unit cell size is increased about 80%, while the wider side size is

the same as the waveguide shown in Fig. 5 because of the waveguide cut-off frequency considerations. Therefore, the waveguide dimension in one direction is reduced considerably and undesirable higher order resonance frequencies near the dominant resonance frequency are eliminated by using lumped capacitors in the FSS structure. The filter bandwidth is less than 2%. Therefore, it is suitable for narrow band applications.

4. CONCLUSION

A new band-pass FSS structure with lumped capacitors suitable for the design of the waveguide filters has been presented. By using lumped capacitors, the waveguide filter dimension is reduced about 80% in one direction compared with the analogous waveguide filter without lumped capacitors. Furthermore several undesirable higher order resonance frequencies near the dominant resonance frequency are eliminated. The future work is designing wideband waveguide filters by using multiple FSSs placed on the transverse plane of the rectangular waveguide.

REFERENCES

1. Konishi, Y. and K. Uenakada, "The design of a bandpass filter with inductive strip-planar circuit mounted in waveguide," *IEEE Trans on Microwave Theory and Tech.*, Vol. 22, No. 9, 839–841, September 1974.
2. Vahldieck, R. and W. J. R. Hoefer, "Finline and metal insert filters with improved passband separation and increased stopband attenuation," *IEEE Trans. on Microwave Theory and Tech.*, Vol. 33, No. 12, 1333–1339, December 1985.
3. Robinson, A. J., R. D. Seager, and J. C. Vardaxoglou, "Waveguide with resonant array inserts," *Electron. Letter*, Vol. 28, No. 23, November 1992.
4. Langley, R. J., "A dual-frequency band waveguide using FSS," *IEEE Microwave Guided Wave Letter*, Vol. 3, No. 1, 9–10, January 1993.
5. Lockyer, D. S. and J. C. Vardaxoglou, "Reconfigurable FSS response from two layers of slotted dipole arrays," *Electron. Letter*, Vol. 32, No. 6, March 1996.
6. Seager, R. D., J. C.Vardaxoglou, and D. S. Lockyer, "Close coupled resonant aperture inserts for waveguide filtering applica-

tions," *IEEE Microwave Wireless Components Letter*, Vol. 11, No. 3, 112–114, March 2001.

7. Monorchio, A., G. Manara, U. Serra, G. Marola, and E. Pagana, "Design of waveguide filters by using genetically optimized frequency selective surfaces," *IEEE Microwave and Wireless Component Letters*, Vol. 15, No. 6, 407–409, June 2005.
8. Martynyuk, A. E., J. Lopez, and N. A. Martynyuk, "Active frequency selective surfaces based on loaded ring slot resonators," *Electronic Letters*, Vol. 41, No. 1, 2005.
9. Roden, J. A., S. D. Jedney, M. P. Kesler, J. G. Maloney, and P. H. Harms, "Time-domain analysis of periodic structures at oblique incidence: Orthogonal and non-orthogonal FDTD implementations," *IEEE Trans. Microwave Theory and Tech.*, Vol. 46, 420–427, 1998.
10. Picket-May, M. J., A. Taflove, and J. Baron, "FDTD modelling of digital signal propagation in 3D circuits with passive and active loads," *IEEE Trans. Microwave Theory and Tech.*, Vol. 42, 1514–1523, 1994.
11. Amjadi, S. M., *Design and Analysis of Frequency Selective Surfaces with Lumped Elements Using Split-field Update FDTD Method*, MSC Thesis, Iran University of Science and Technology, January 2007.